A New Correlation to Estimate Bearing Capacity of Micropile Groups

A. Ghanbari, M. Yoosefi Taleghani[*]

Faculty of Engineering, Kharazmi University, Tehran, Iran

ABSTRACT: Most of the recent studies that have focused on the micropile group have been limited to a specific soil type. However, the bearing capacity of micropile groups has not been considered in any of these studies. This study concerned three-dimensional numerical modeling of loose sand, medium sand, silty clay, and soft clay improved by the micropile group. The bearing capacity of the micropile group was estimated by 3D numerical modeling. The micropile group was modeled using spacing to diameter ratio (S/D) and the ratio of micropile length to cap width of micropile (L/B) in soil. Despite the use of only the shear failure criterion in the FHWA Code, the allowable settlement criterion was also considered in this study. A novel approach was presented to estimate the bearing capacity of the micropile group in which a new concept known as "unit length bearing capacity" has been used for the first time. The results demonstrated that in all four soils studied, the unit length bearing capacity of the group will decrease with increasing micropile length. In addition, the settlement of the micropile group in all four soils will decrease with increasing micropile length. The unit length bearing capacity of the micropile group and the overall bearing capacity of the micropile group in all four soils will decrease with an increasing spacing of micropiles. Of course, with increasing micropile length, the unit length bearing capacity will decrease at a slower rate than the overall bearing capacity. According to the simulation results, a punching failure occurred in the micropile group.

1- Introduction

The two common methods to deal with problematic soils are: (1) the use of load-bearing elements (LBEs) and (2) the injection of materials to improve the strength parameters of the soil. Slurry injection influences soil improvement (Ghadimi et al. 2017). Micropiles include the advantages of both methods. A micropile refers to a pile with a diameter less than 300 mm which is commonly associated with light steel reinforcement and cement slurry injection. The arrangement of micropiles is dependent on the position of foundations and columns, geometrical and structural characteristics of the foundation, strength parameters and bearing capacity of the soil, and micropile depth.

With liquefaction and reduction of shear strength of soil, large settlements are imposed on shallow foundations of buildings which may, in turn, cause serious damage to the structure and non-structural elements and ultimately destruction of buildings. On the other hand, the bearing capacity of columns on the foundation and load transfer to deeper layers are determinant factors in some civil projects irrespective of executive and economic issues. In general, a micropile prevents liquefaction and provides bearing capacity of columns on the foundation, and transfers the load to deeper layers. Recently, studies have been conducted on inclined micropiles

(Sadek, et al. 2006), settlement of hollow-bar micropile group (Abd Elaziz and El Naggar 2014), bending stiffness of micropile group (Abdollahi and Mortezaei 2015), cyclic bearing capacity of micropile group (Matos, et al. 2015), uplift and lateral bearing capacity of micropile group (Kyung and Lee 2017; Kyung and Lee 2018), reduction of liquefaction risk by micropile group (Schultz, et al. 2019), determining shaft bearing capacity of semi-deep foundations socketed in rocks (Rezazadeh and Eslami 2017), the efficiency of micropile groups (Sharma, et al. 2019), Evaluation of the performance of piled-raft foundations on soft clay (Khanmohammadi and Fakharian 2018), Analysis of load sharing characteristics for a piled raft foundation (Ko, et al. 2018) and Response of passively loaded pile groups (Al-abboodi, et al. 2020). Most studies have focused on a specific soil type, not several soil types. On the other hand, no correlation has been suggested for calculating the bearing capacity of micropile groups in several soil types.

In the current study, in addition to the bearing capacity of the micropile group in four soil types, a new approach was proposed to calculate the bearing capacity of the micropile group. Through 3D numerical analysis, a new correlation is presented with a different approach for estimating the bearing capacity of the micropile group based on an allowable settlement of 1" (25.4 mm). This correlation can estimate

*Corresponding author's email: mahdi.yusef.t@gmail.com

the bearing capacity of the micropile group embedded in four soils using an innovative concept known as "unit length bearing capacity".

2- Literature Review

Reviewing recent studies on micropile groups, it is observed that most studies have focused on non-cohesive soils. Load-settlement curves have been considered in most studies.

Sadek et al. (2006) numerically studied the effect of micropile inclination on the performance of a micropile network. According to their results, micropile inclination reduced axial force and thereby increased the bearing capacity of the micropile group. Under lateral loading, it caused an increase in lateral stiffness while reducing both shear force and bending anchor in micropiles. However, they did not investigate the effect of the number and spacing of micropiles on the bearing capacity of the micropile group.

Abd Elaziz and El Naggar (2014) studied the group behavior of hollow-bar micropiles in cohesive soils through large-scale field experiments and 3D numerical modeling. They proposed a method to calculate the settlement of the micropile group and a series of curves to calculate the interaction of micropiles. However, the bearing capacity of the micropile group and the effect of several micropiles on the settlement of the micropile group have not been investigated in this study.

Abdollahi and Mortezaei (2015) evaluated the bending stiffness of circular micropile groups through numerical simulation. The effect of number, diameter, length, angle and injection pressure of micropiles on reaction modulus of bed and bearing capacity of micropile group was studied. A new correlation was suggested to evaluate the bending stiffness of the micropile group. Only a micropile group with a circular arrangement was studied and no correlation was presented for evaluating the bearing capacity of the micropile group.

Matos et al. (2015) experimentally studied the behavior of single and group micropiles on loose sand under controlled conditions. The effect of cyclic loading on the behavior of micropiles and slurry injection on improved strength of micropiles and mechanical properties of soil was evaluated and load-settlement curves were plotted. However, only loose sandy soil was tested and the bearing capacity of the micropile group was not evaluated.

Alnuaim et al. (2016) studied a numerical investigation of the performance of micropile rafts in the sand. In this study, a calibrated and verified finite element model (FEM) with centrifuge tests was used to carry out a numerical investigation of the performance of MPR in the sand. The micropile raft (MPR) offers an efficient foundation system that combines the advantages of micropiles and piled rafts that can be used as a primary foundation system or to enhance an existing raft foundation. The outcomes of this investigation helped in understanding the effect of these factors on the MPR axial stiffness, including; differential settlement; load sharing between the MPs and the raft; and the raft bending moment. Moreover, the ability of the PDR method to evaluate the axial stiffness

of an MPR for the preliminary design stage was examined.

In another study, Alnuaim et al. (2018) also studied a numerical investigation of the performance of micropile rafts in clay. In this study, a finite element model (FEM) calibrated and verified with centrifuge tests was used to carry out a numerical investigation of the performance of MPR in clay. The outcomes of this investigation helped in understanding the effect of these factors on the MPR axial stiffness, including; differential settlement; load sharing between the MPs and the raft; the raft bending moment, and micropiles skin friction. Moreover, the ability of the Poulos-Davis-Randolph (PDR) method to evaluate the axial stiffness of an MPR for the preliminary design stage was examined.

Kyung and Lee conducted two studies on micropiles. In the first study (Kyung and Lee 2017), the uplift bearing behavior of micropiles in silty sand and soft clay was investigated by testing the model and large-scale experiments, and the effect of various installation conditions in terms of installation angle (θ) and spacing of micropiles (S) and micropile group geometry was studied. In the second study (Kyung and Lee 2018), the effect of micropile inclination was examined through numerical analysis, testing the model and large-scale experiments on the lateral bearing capacity of micropile group in silty sand under different conditions in terms of micropile inclination angle (θ), load inclination angle (δ) and spacing of micropiles (S) in silty sand. In both studies, uplift and lateral bearing capacity of the micropile group were studied, but the bearing capacity of micropiles was not evaluated.

Schultz et al. (2019) experimentally studied the possibility to use a micropile group under the foundation of a school in California to reduce the risk of liquefaction. The micropile group was tested under combined axial and lateral forces. According to their results, the micropile group was able to reach a significant bearing capacity and reduce the risk of liquefaction. A specific soil type was considered and the bearing capacity was not evaluated.

Sharma et al. (2019) experimentally studied the effect of parameters affecting the efficiency of micropile groups installed in sandy soils. The effect of length and spacing of micropiles in the group and relative compaction of soil on the performance of the micropile group was studied. However, the effect of several micropiles was not evaluated. Only sandy soils were studied and other soil types were not considered. The bearing capacity of the micropile group was not evaluated.

Abdlrahem and El Naggar (2020) studied the axial performance of micropile groups in cohesionless soil from full-scale tests. Hollow bar micropile (HBMP) groups are used for supporting large loads as an alternative foundation option to large diameter drilled shafts. In this study, the effect of increasing Db and micropile spacing on the group performance was investigated experimentally and numerically. The results demonstrated that micropile groups constructed with the large diameter drill bits displayed higher stiffness and load-carrying capacity than the groups constructed with small diameter bits, which confirms the effectiveness of using a larger drill bit. In addition, the group efficiency ratio values
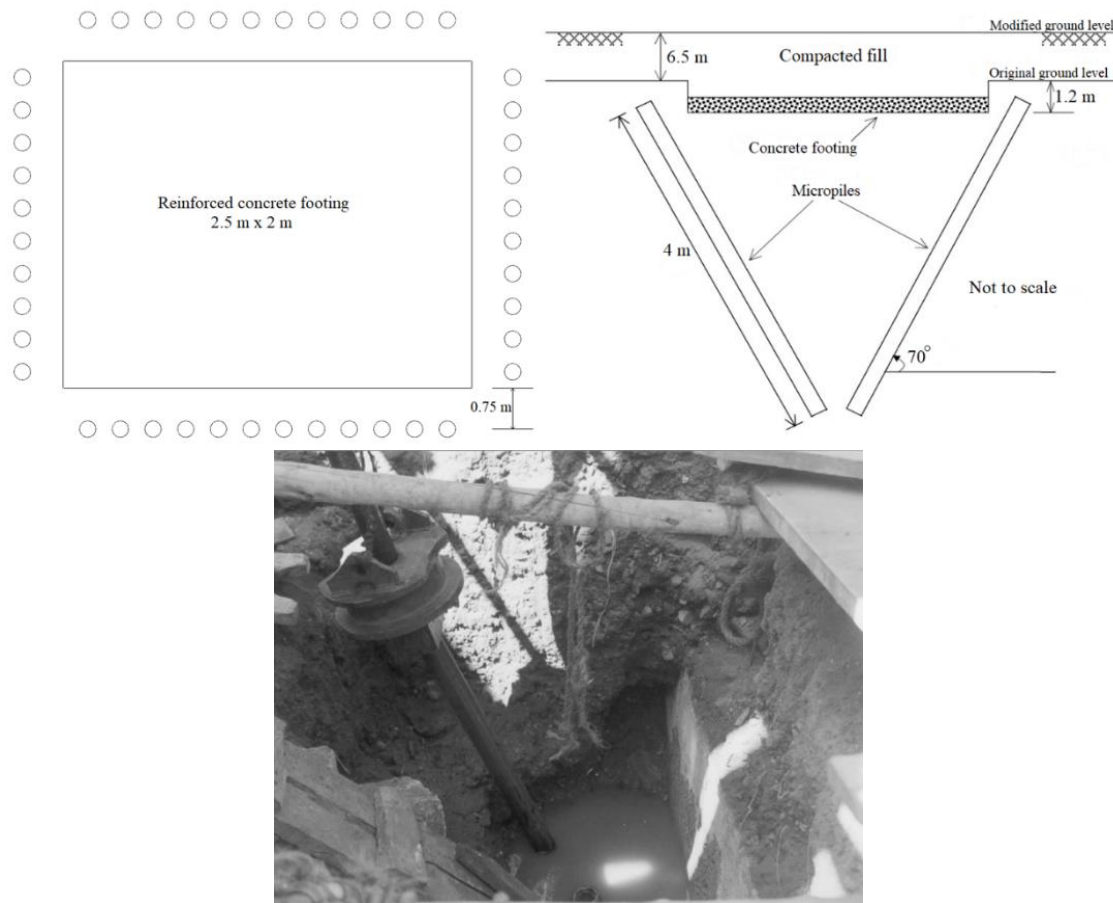
Fig. 1. Plan and cross-section of the micropile group and micropiling at the site studied by Babu et al. (2004).

at both working load and ultimate capacity were found to be close to unity for all groups.

Bayesteh and Fakharnia (2020) studied a numerical simulation load test on hollow-bar micropiles by considering the grouting method. This study used finite element modeling of full-scale loading tests on hollow-bar micropiles in coarse-grained and fine-grained soil to evaluate their design parameters and the effect of the grouting method.

According to the literature on micropile groups, one of these studies has investigated the simultaneous effect of the length, number, and spacing o micropiles and soil type. While evaluating all these factors, a novel method is proposed for determining the bearing capacity of micropile groups. For the first time in this study, a new concept known as "unit length bearing capacity of micropile group" is introduced. In this novel method, a new correlation is presented for calculating the bearing capacity of the micropile group in four soil types.

3- Numerical Analysis

Four soil types were numerically analyzed with the help of MIDAS GTS NX finite element software. To select soil type, all soils used in the micropile group are considered as effective load-bearing members. To this end, loose sand, medium sand, silty clay, and soft clay were considered.

3- 1- Validation

The results of Babu et al. (2004) were used for validation of modeling results. Fig. 1 shows a schematic of the micropile group and micropiling at the site studied by Babu et al. (2004). This study deals with a case study in which micropiles of 100 mm in diameter and 4 m long have been used to improve the bearing capacity of foundation soil and in the rehabilitation of the total building foundation system. The settlement of a 3×3 micropile group with a length of 3 m embedded in loose sandy soil and the results of Babu et al. (2004) are shown in
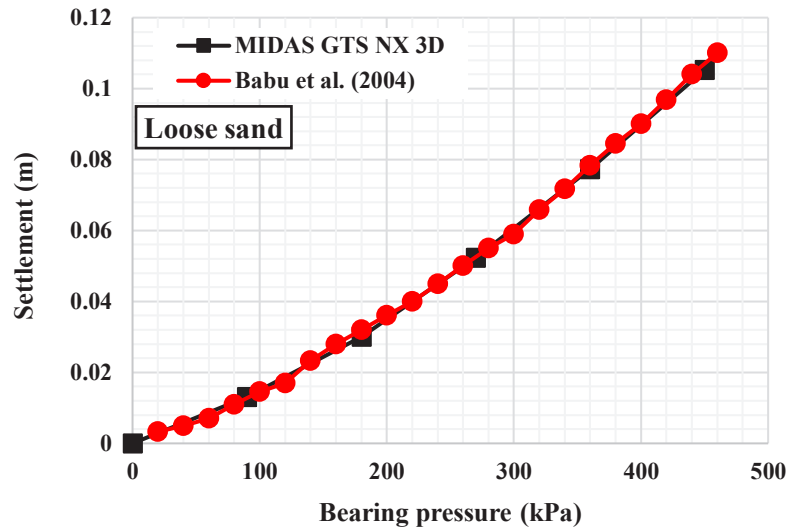
Fig. 2. Comparison of numerical results of this study with numerical- case study results of Babu et al. (2004) for loose sandy soil.

Table 1. Characteristics of soil and micropile studied by Babu et al. (2004).

Material	ϕ (Degrees)	c (kPa)	E (kPa)	Poisson's Ratio	γ (kN/m^3)
Loose Sand	25	1	13000	0.30	18.0
Micropile	-	-	210000	0.25	78.5

Fig. 2. Table 1 lists soil and micropile characteristics.

As can be seen, the results of 3D analysis by MIDAS are relatively consistent with those reported by Babu et al. (2004). The bearing capacity per 1in (25.4 mm) settlement obtained numerically and case study (Babu et al. 2004) is 160 and 150 kPa, respectively, which are very close to each other.

3- 2- Geometrical Specifications of Models and Materials Characteristics

To evaluate the behavior of the micropile group, numerical models were analyzed for 3×3, 5×5, and 10×10 micropiles with an S/D ratio of 3, 5, and 10 (S: spacing of micropiles and D: micropile diameter=0.1) and an L/B ratio of 0.5, 1, 2 and 4 (L: micropile length, B: cap width) in silty clay, soft clay, loose sand, and medium sand. Figs. 3 and 4 schematically show the model and boundaries. The width of the soil medium is extended 2 times of foundation width (2B) around the concrete foundation, i.e. soil medium width equals 5B. The depth of the soil medium is extended two times the micropile length (2L). Characteristics and variables used in the models are presented in Table 2.

As mentioned, loose sand, medium sand, silty sand, and soft clay were numerically modeled. Table 3 presents the characteristics of these soils.
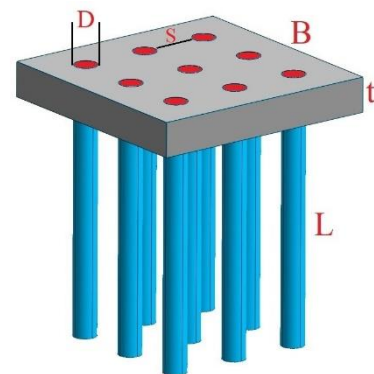
Fig. 3. Schematic representation of the micropile group and its dimensions used in this study.
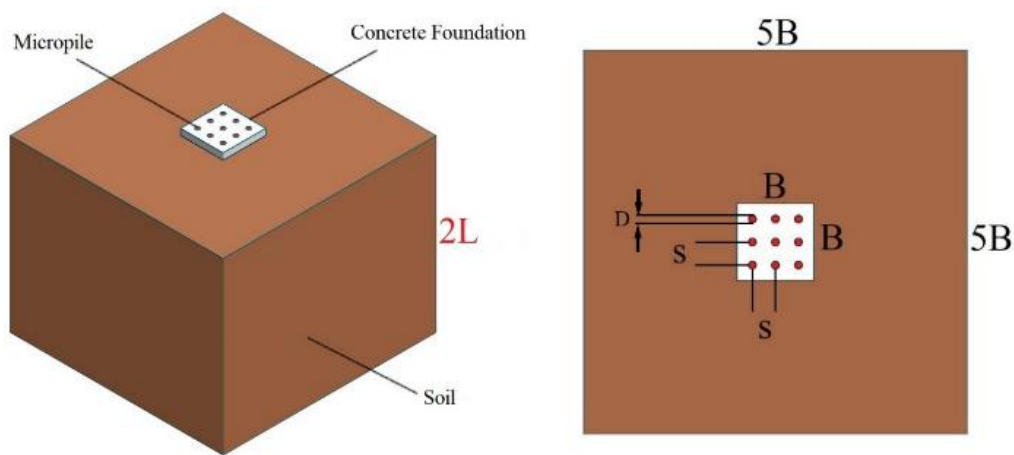
Fig. 4. Schematic representation of the models and boundaries in this study.

Table 2. Characteristics and variables of the models used in this study

Soil Type	Silty clay, soft clay, loose sand, medium sand
Modeling of structural elements	Three-dimensional
Number of micropiles in the group, *n*	9, 25, 100
S/D ratio	3, 5, 10
Diameter of micropile, *D*	0.1 m
L/B ratio	0.5, 1, 2, 4
Thickness of cap, *t*	0.05B

Table 3. Geotechnical characteristics of studied soils (Verbrugge & Schroeder, 2018).

Soil Type	c_u (kPa)	ϕ (Degrees)	c (kPa)	E (kPa)	Poisson's Ratio	γ (kN/m^3)
Loose Sand	0	30	0	18000	0.30	17.0
Medium Sand	0	35	0	40000	0.35	19.5
Silty Clay	50	25	30	25000	0.35	18.0
Soft Clay	60	20	40	10000	0.40	15.0

Table 4 shows the characteristics of materials used in micropiles, slurry, and concrete foundations.

To consider the effect of slurry injection in soil, the cemented soil around each element with a radius of 2D=20 cm was assumed. According to the literature on cemented soils, c and ϕ increase in this range of model soil. As a result of soil cementation, its behavior changes from granular to cohesive soil. In a granular soil, friction angle does not change significantly with increasing cement content, but cohesion increases significantly. The same is true for cohesive soils. With increasing cement content, friction angle first increases and then remains almost constant. However, cohesion increases significantly. Amini et al. (2014) presented a correlation for an increase in ϕ of cemented granular soils in Eq. (1):

$$\left(\phi_{CV}\right)_{cemented} - \left(\phi_{CV}\right)_{uncemented} = 8.3° + 0.013D_r \quad (1)$$

Table 4. Characteristics of micropiles, slurry, and concrete foundation (Verbrugge & Schroeder, 2018)

Parameter	Content	Unit
Unit weight of concrete	25	kN∕m^3
Young's modulus of concrete	21000	MPa
The Poisson's ratio of concrete	0.18	_
Unit weight of the bar	78	kN∕m^3
Young's modulus of bar	200000	MPa
Unit weight of grout	11.10	kN∕m^3
Young's modulus of grout	31000	MPa

Table 5. Internal friction angle of cemented soils used in this study.

Soil Type	$(\phi)_{cemented}$ (Degrees)
Loose Sand	38
Medium Sand	43
Silty Clay	29
Soft Clay	24

Table 6. The cohesion of cemented soils used in this study.

Soil Type	$(c)_{cemented}$ (kPa)
Loose Sand	150
Medium Sand	150
Silty Clay	130
Soft Clay	140

where $(\phi_{CV})_{uncemented}$ and $(\phi_{CV})_{cemented}$ respectively represent the internal friction angle of the soil before and after cementation and Dr is the relative density of soil. The term 0.013Dr is negligible and eliminated. Thus, in granular soils, the internal friction angle increases by 8° after cementation. As previously mentioned, the same is true for cohesive soils. However, the increase in internal friction angle of cemented cohesive soils is considered to be 4° (half that of granular soil) through engineering judgment. By adding these values to the internal friction angle in Table 3, the resultant Table 5 is obtained.

Haeri et al. (2005) presented a diagram for estimating the increased unconfined compressive strength of cemented granular soils. According to this diagram, the lowest unconfined strength of 600 kPa is obtained at a cement content of 3%. The undrained cohesion of granular soil equals half of the unconfined strength (300 kPa). It is assumed that the cohesion of granular soils increases by 150 kPa. As mentioned, the same holds for cohesive soils. However, according to engineering judgment, two-thirds of 150 kPa, i.e. 100 kPa, was considered as an increase in cohesion of cemented cohesive soils. Fine-graded soils yield a substantial increase in cohesion and less improvement in internal friction angle (Thompson 1966, Muhunthan and Sariosseiri 2008). This statement indicates that stabilization displays brittle behavior. Cement-treated soils exhibit a significant increase in compressive strength under the UCS test, which varies from 40 times for fine-graded soils to 150 times for coarse-graded soils (Mitch-

ell 1976). Therefore, to judge the cohesion of fine-grained soil stabilized with cement, engineering judgment has been used in the mentioned range. By adding these values to cohesion values in Table 3, the resultant Table 6 is obtained.

Micropiles were defined as an isotropic elastic medium of a structure type with specifications listed in Table 4. Each micropile includes slurry and reinforcement rebar. A combined cross-section was defined for modeling micropiles, and equivalent density and modulus of elasticity of combined cross-section were used.

According to FHWA-NHI-05-039, the equivalent axial stiffness of micropile is obtained from Eq. (2). The equivalent modulus of elasticity of the combined cross-section is obtained accordingly (Sabatini et al. 2005).

$$[E.A]_{micropile} = [E.A]_g + [E.A]_s \qquad (2)$$

According to FHWA-NHI-05-039, the ultimate shear force is obtained from Eq. (3) (Sabatini et al. 2005):

$$UltimateShearForce = \frac{\alpha_{bond}}{F_s} \qquad (3)$$

Table 7. Cohesion of cemented soils used in this study.

	α_{bond} (kPa)	UltimateShearForce (kPa)
Soft Clay	97.5	48.75
Silty Clay	142.5	71.25
Loose Sand	167.5	83.75
Medium Sand	265.0	132.50

where α_{bond} represents the ultimate bond strength of slurry and ground in terms of kPa and is selected according to Table 7, F_s is the reliability coefficient and equals 2. The slurry is injected by method D. The ultimate shear force of micropiles calculated from Eq. (3) is presented in Table 7.

Moduli of shear ($K_{t\,(kN/m^3)}$) and normal ($K_{n\,(kN/m^3)}$) stiffness are respectively calculated by Eqs. (4) and (5) (Datta 2010):

$$K_t = \frac{G.S_u.L}{MicropileArea} \qquad (4)$$

$$K_n = \frac{G.S_w.L}{MicropileArea} \qquad (5)$$

where G is the shear modulus of soil, L micropile length, and S_u and S_w represent resilient moduli of soil (Datta 2010).

3- 3- Micropile Modeling

Micropiles were modeled three-dimensionally using the Mohr-Coulomb failure criterion with specifications presented in section 3.2.

To define and assign properties to materials, the "Property" option in the "Mesh" tab was used. Soil, cement, and concrete elements are defined as "Solid" three-dimensional elements. The micropile element is defined as a "Beam" one-dimensional element with a solid circular cross-section with a diameter of 0.1 m. The interface element is defined as a one-dimensional "Pile" element with a thickness of 0.1 m. The "Other" element of the "Pile Tip" type has been used to model the bearing capacity of the tip and the spring stiffness of the tip.

In this research, four zones have been considered for modeling each micropile. As shown in Fig. 5, the first zone has been defined as including the grout and reinforcing bar, of the one-dimensional beam element type with a filled-circle section with a diameter of 0.1 m as a composite section. The second zone is the steel casting zone, of the one-dimensional interface pile element type with a thickness of 0.1 m, where
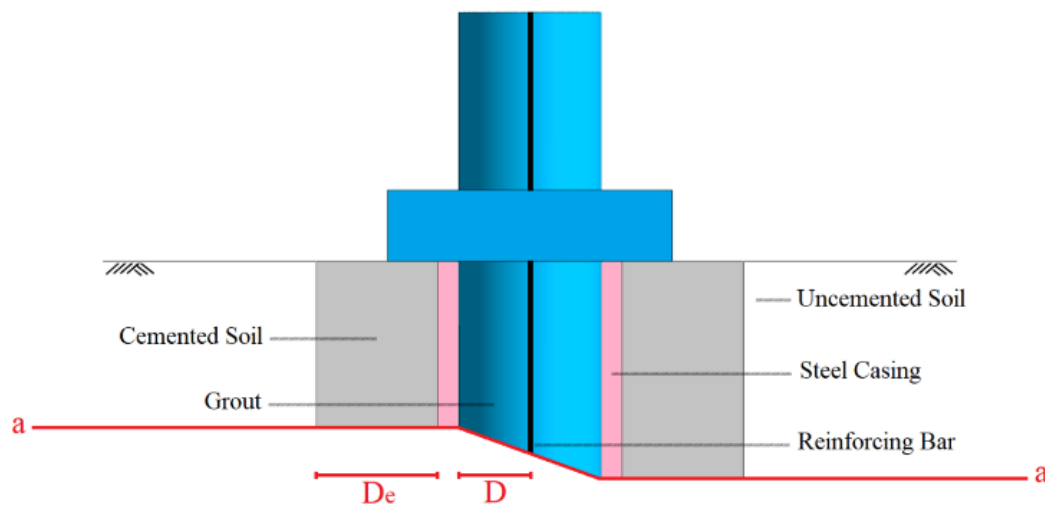
Fig. 5. Schematic of the longitudinal section of the modeled micropile.
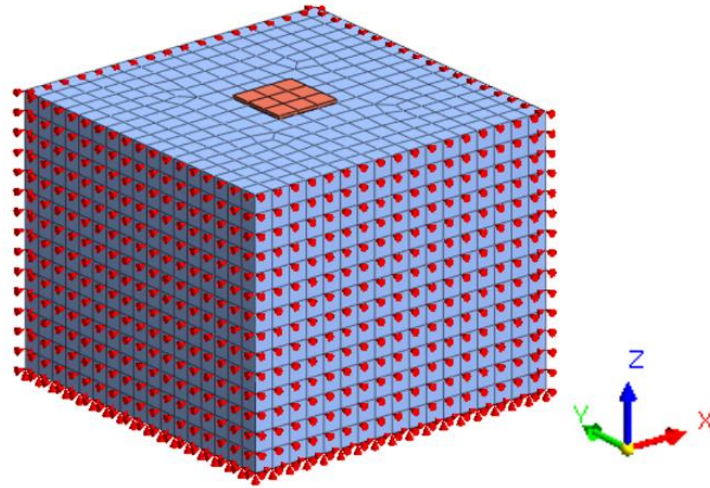
Fig. 6. Boundary conditions and micropile group in MIDAS GTS NX.
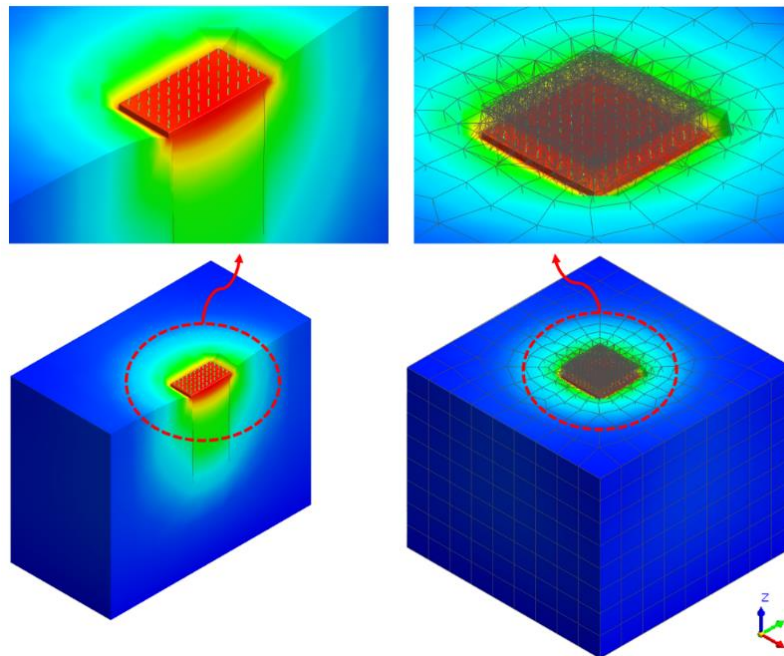
Fig. 7. The finite element grid and vertical deformation contours of the micropile group with a height of 20.4 m in silty clay modeled with the help of MIDAS GTS NX.

the values of ultimate shear force, shear stiffness modulus (K_t), and normal stiffness modulus (K_n) have been set. The third and fourth zones are uncemented soil and cemented soil, respectively, defined as the three-dimensional solid element type. In this research, the idea of cemented soil zone has been used for modeling the soil injected around the micropile, while this zone had not been defined in the same way in the previous studies. The thickness of the cemented soil zone is referred to as the "radius influence of the injection zone," represented by D_e. Experience has shown that the radius influence of the injection zone does not usually exceed twice the micropile radius; therefore, the value of D_e in this research has been assumed to be 2D. Moreover, the micropile tip ex-

hibits little resistance, the impact of which has been defined using the pile tip element, where the values of tip bearing capacity and tip spring stiffness have been set.

Appropriate boundary conditions should be defined for model stability and determination of stiffness matrix. Simple far boundaries are usually used in static analyses. To this end, as shown in Fig. 6, the sides are along the X- and Y-axes and the bottom side along the Z-axis.

After simulation, the model is analyzed. Fig. 7 shows the finite element grid and vertical deformation contours of the micropile group with a height of 20.4 m in silty clay modeled with the help of MIDAS.

4- Results and Discussion

The effects of the micropile group on foundation settlement and load-settlement curve of the micropile group were analyzed with the help of MIDAS. The 3D models were developed using the Mohr-Coulomb failure criterion. Fig. 8 shows the load-settlement curves of micropile groups in silty clay, soft clay, loose sand, and medium dense sand. In these diagrams, 3×3 means a micropile group consisting of 9 micropiles, 5×5 means a micropile group consisting of 25 micropiles, and 10×10 means a micropile group consisting of 100 micropiles. Moreover, L, B, S, and D represent the length, cap width, spacing, and diameter of micropiles, respectively.

(a) loose sand

(b) medium dense sand

(c) silty clay
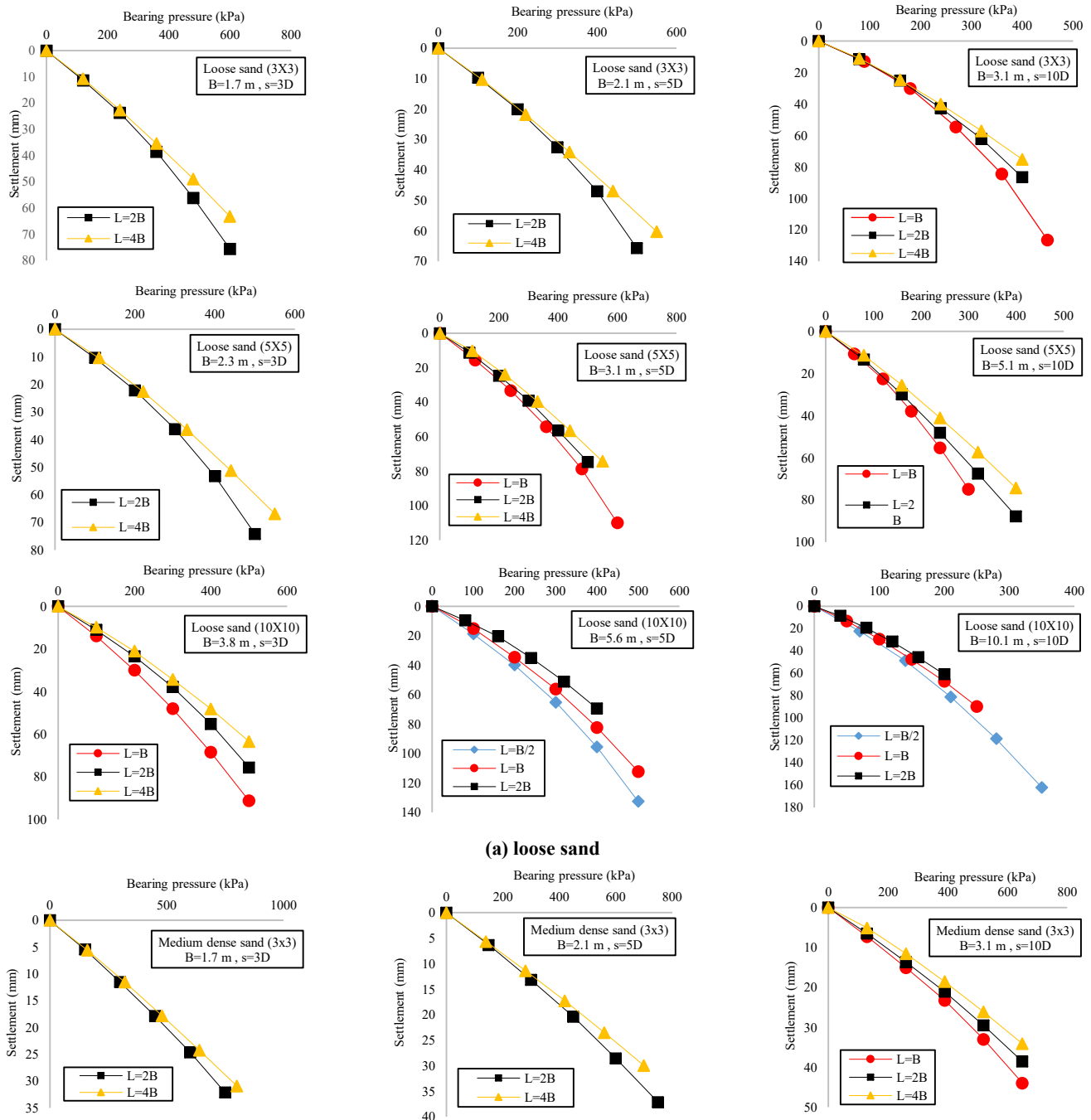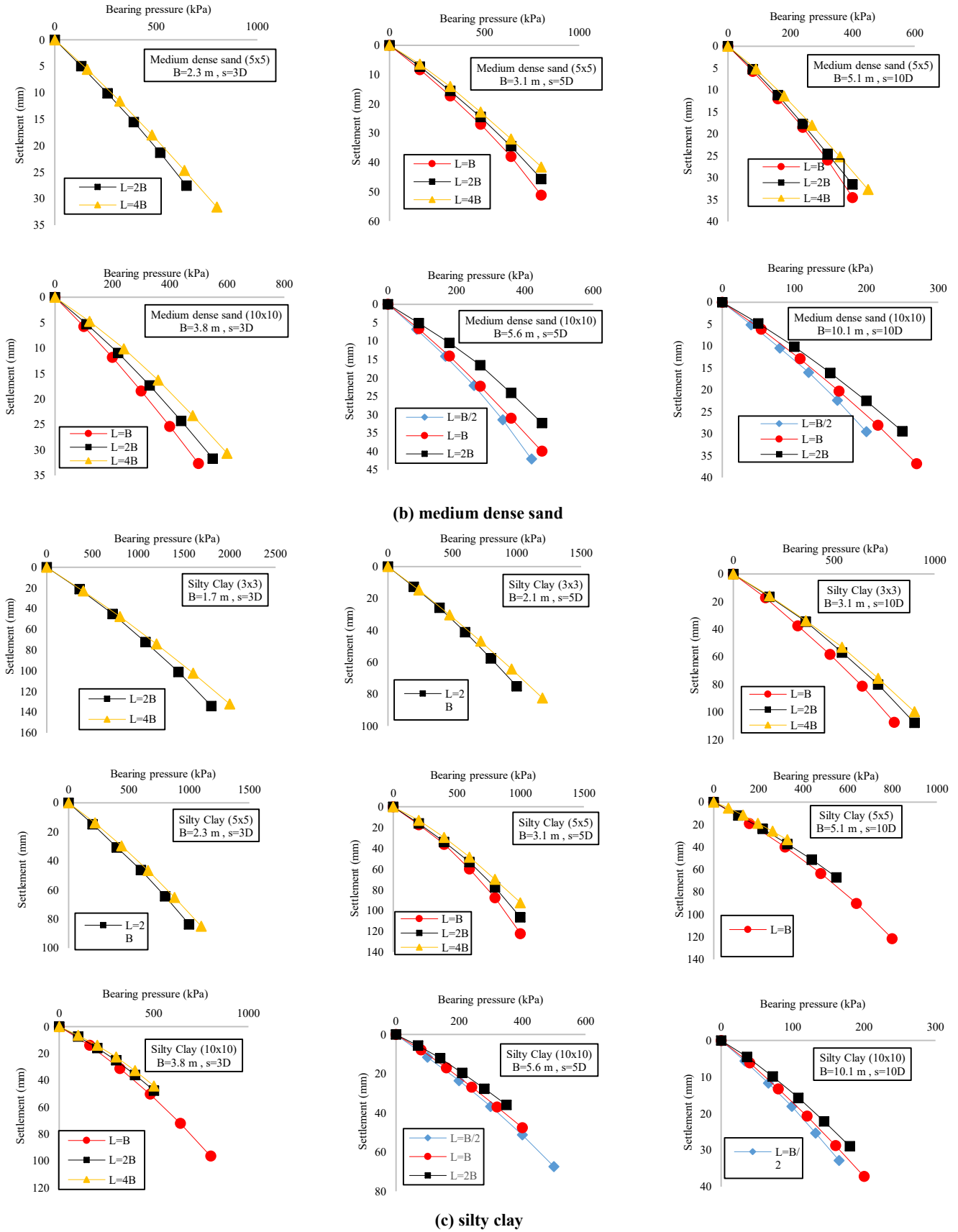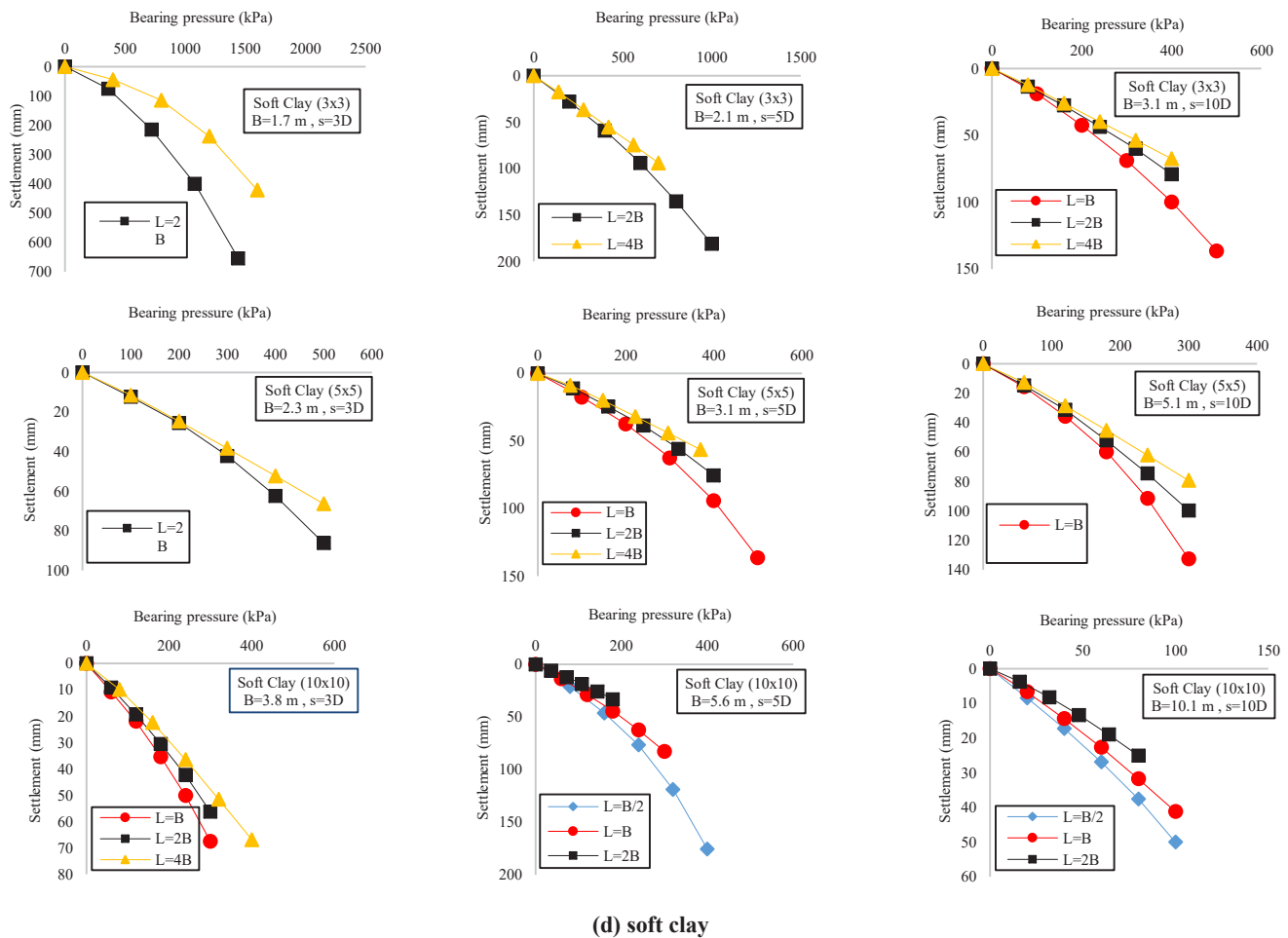
Fig. 8. Load-settlement curves of micropile groups.

As clearly seen, with increasing the micropile length, the settlement of the micropile group decreases, and an upward trend is observed.

To study the effect of length (L/B), spacing (S/D), and number (n) of micropiles on the bearing capacity of the micropile group, the unit length bearing capacity versus 1in (25.4 mm) allowable settlement was obtained from Fig. 8 and was presented in terms of these parameters (Fig. 9).

As can be seen from the trend of the curves in Fig. 9, in all curves, with increasing the S/D ratio, the unit length bearing capacity has decreased. Of course, with increasing the length

of micropiles (increasing the L/B ratio), the unit length bearing capacity has decreased at a slower rate. Therefore, it can be concluded that with increasing the distance of micropiles in the group, the unit length bearing capacity will always decrease.

By performing mathematical analysis on the coefficients of trendline equations fitted to the curves of Fig9 . by Excel software, a formula was obtained for calculating the unit length bearing capacity of the micropile group in loose sand, medium sand, silty clay, and soft clay as a function of dimensionless parameters of spacing (S/D), length (L/B)

(a) loose sand

(b) medium dense sand
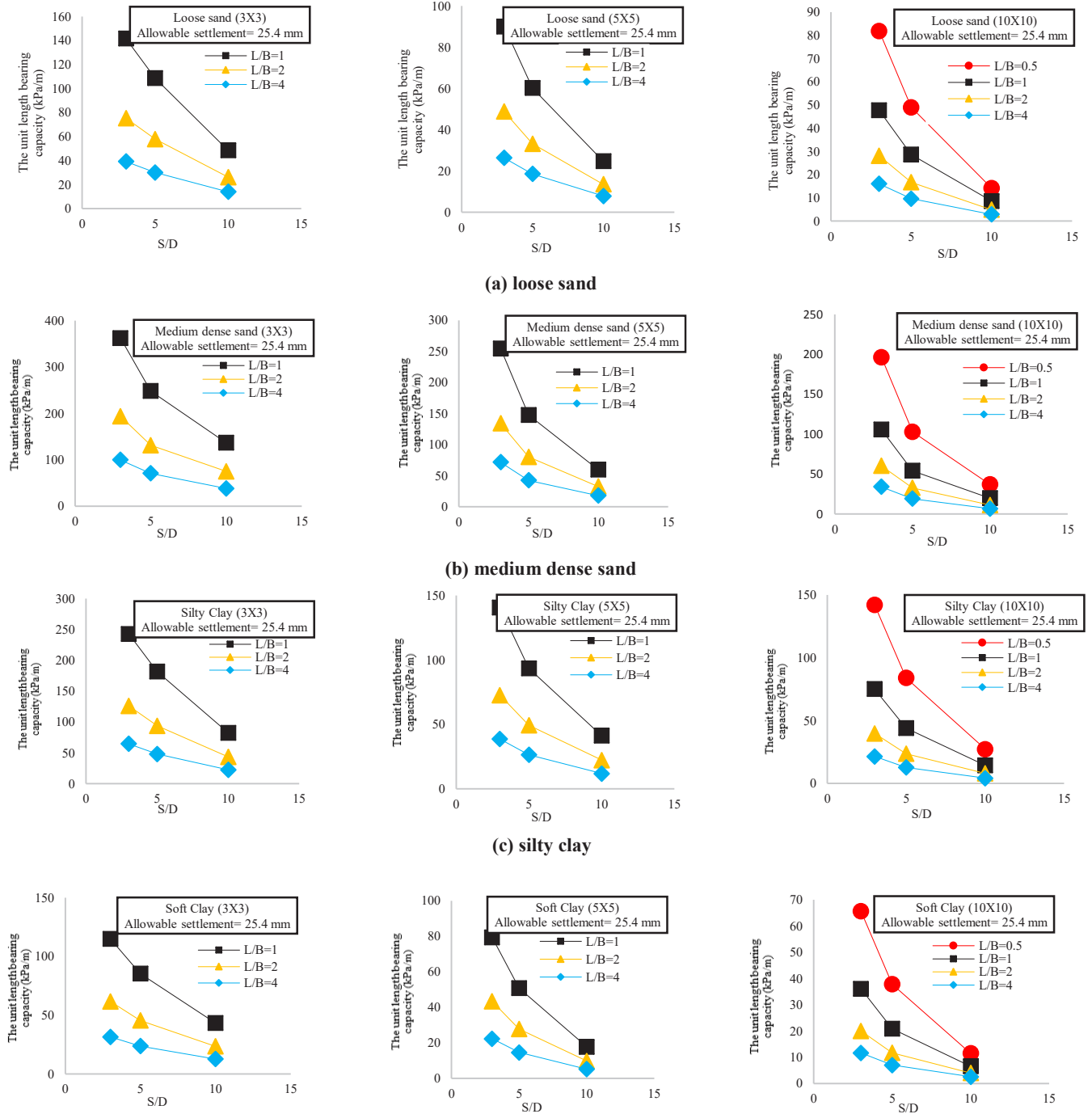
(c) silty clay

Fig. 9. The unit length bearing capacity of micropile groups, allowable settlement= 25.4 mm.

Table 8. Bearing capacity coefficients of the micropile group.

Coefficient (kN/m^3)	Loose sand	Medium sand	Silty clay	Soft clay
a	-8	-20	-13	-6
b	57	143	94	45
c	16	40	28	12
d	-107	-273	-182	-86
e	27	68	44	21
f	-173	-439	-289	-140
g	-52	-136	-91	-42
h	327	841	523	268
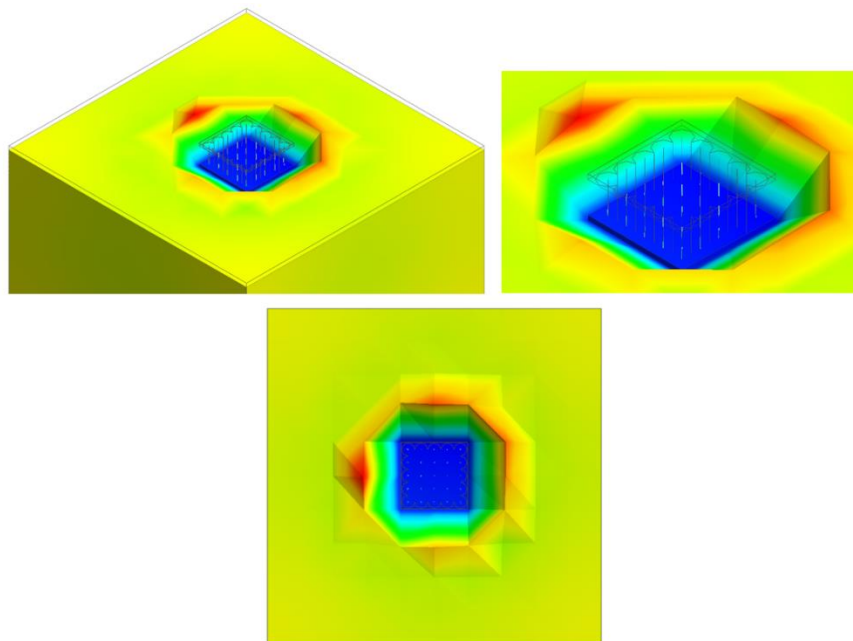
Fig. 10. Local failure of the micropile group in MIDAS.

and number (n) of micropiles. The proposed correlation for calculating the bearing capacity of micropile groups is obtained by multiplying micropile length (L) by the resulting formula (Eq. (6)):

$$
(BC)_g = \left[\begin{array}{l} \{a \ln(n) + b\}.\ln\left(\dfrac{L}{B}\right).\ln\left(\dfrac{S}{D}\right) + \\[2mm] \{c \ln(n) + d\}\ln\left(\dfrac{S}{D}\right) + \\[2mm] \{e \ln(n) + f\}\ln\left(\dfrac{L}{B}\right) + g \ln(n) + h \end{array} \right].L \quad (6)
$$

where $(BC)g$ represents the bearing capacity of the micropile group, n number of micropiles in the group, S spacing of micropiles, D micropile diameter, L length of micropiles and B is the width of micropile cap. The coefficients a, b, c, d, e, f, g, and h for four soils are presented in Table 8.

5- Comparison of Results by FHWA, Meyerhof, and Vesic Methods

The bearing capacity of the micropile group was extracted based on an allowable settlement of 1in (25.4 mm) Analyses were performed in such a way that the settlement of the micropile group does not exceed a few inches. This leads to a local failure (punch) in the micropile group. Fig. 10 shows an example of local failure.

697
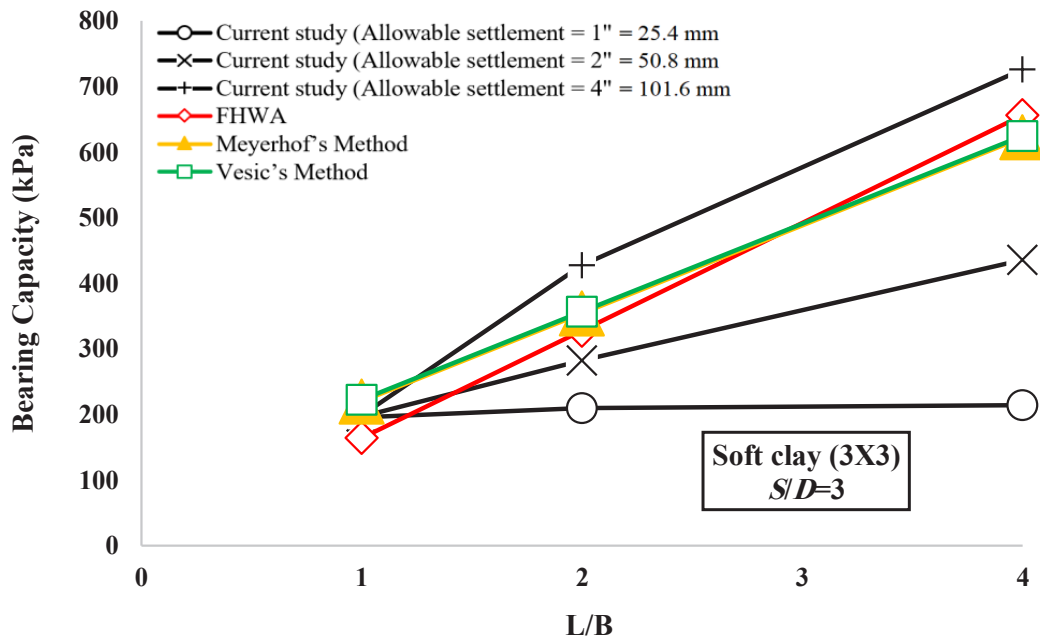
Fig. 11. Comparison of bearing capacities of the micropile group calculated by different methods.

However, the bearing capacity of the micropile group in FHWA, Meyerhof (1976), and Vesic (1977) methods is calculated based on the shear failure and a general failure is assumed in these methods.

Eq. (6) is proposed for evaluating the bearing capacity of the micropile group based on 1in (25.4 mm) allowable settlement. However, the bearing capacity of the micropile group is calculated based on shear failure in FHWA, Meyerhof, and Vesic methods, not based on this settlement criterion. Accordingly, the bearing capacity obtained from these methods is often higher than that calculated by the formula proposed in this study. For small micropile lengths, the bearing capacity evaluated by these methods is very close to that obtained in this study. This indicates the occurrence of shear failure at 1in (25.4 mm) settlement at small micropile lengths. Fig. 11 compares the bearing capacity of a 3×3 micropile group with S/D=3 buried in soft clay based on FHWA, Meyerhof, and Vesic methods and also Eq. (6). The method was used to calculate frictional (shell) bearing capacity in Meyerhof and Vesic methods (Terzaghi et al. 1996).

As can be seen in Fig. 11, the bearing capacity faster increases by increasing micropile length in FHWA, Meyerhof, and Vesic methods than 1in (25.4 mm) allowable settlement. When the bearing capacity of the micropile group is calculated based on the shear failure criterion without settlement limitation, the increase in the micropile length plays its actual role in increasing the bearing capacity. In the absence of settlement limitation, in large displacements which ultimately lead to soil failure, the frictional resistance of the micropile

wall is completely activated in contact with its surrounding soil. This in turn causes a faster increase of bearing capacity in FHWA, Meyerhof, and Vesic methods than 1in (25.4 mm) allowable settlement. Furthermore, when the allowable settlement changes from 1in (25.4 mm) to 2in (50.8 mm) and then 4in (101.6 mm) the bearing capacity evaluated in this study is close to that calculated by FHWA, Meyerhof, and Vesic methods and slope increases. With increasing allowable settlement to 2in (50.8 mm) and 4in (101.6 mm), the frictional resistance of the micropile wall in contact with its surrounding soil is gradually activated. At an allowable settlement of 4in (101.6 mm), the frictional resistance of the micropile wall is fully activated. Consequently, the bearing capacity evaluated based on the shear failure criterion is almost equal to that in FHWA, Meyerhof, and Vesic methods.

6- Conclusion

The behavior of the micropile group was studied under static loading in loose sand, medium sand, silty clay, and soft clay soils. The unit length bearing capacity for these four soils was plotted versus S/D, L/B, and n dimensionless parameters. Using these diagrams, a correlation was derived for calculating the bearing capacity of the micropile group in these four soils as a function of the above-mentioned dimensionless parameters. The main results are presented below.

- A new concept entitled "unit length bearing capacity of micropile group" was introduced. To calculate the overall bearing capacity, this parameter is multiplied by micropile length.

▪ The Eq. (6) correlation was proposed to calculate the bearing capacity of the micropile group for four soils in this study:

▪ In all four soils studied, the unit length bearing capacity of the group decreased, and overall bearing capacity increased with increasing micropile length.

▪ The settlement of the micropile group in all four soils decreased with increasing micropile length.

▪ With the increasing spacing of micropiles, the unit length bearing capacity of the micropile group and the overall bearing capacity of the micropile group in all four soils decreased with an increasing spacing of micropiles. With increasing micropile length, the unit length bearing capacity decreased at a slower rate than the overall bearing capacity.

▪ With increasing the number of micropiles in the group, the unit length bearing capacity and overall bearing capacity of the micropile group in all four soils decreased. The reduction of bearing capacity was further highlighted with decreasing micropile length.

▪ Compared to classical methods, such as Meyerhof (1976), and Vesic (1977), as well as the FHWA method, since the calculation of bearing capacity in these methods is based on the shear failure criterion, therefore the amount of bearing capacity obtained according to the mentioned methods is more than the amount estimated according to the relationship proposed in the current study. However, at low micropile lengths, because of shear failure at the 1in (25.4 mm) settlement, the amount of bearing capacity obtained according to the above methods and the amount estimated according to the relationship proposed in the current study, will be close together.

▪ Using the relationship presented in the current study will be useful in examining the serviceability of projects as well as in examining projects in which we face settlement limitations.

References

[1] M. R. Thompson, Shear strength and elastic properties of lime-soil mixtures, 139: 1-14, Highway Research Record, Washington D.C., 1966.

[2] J. K. Mitchell, The properties of cement-stabilized soils, 365–404, Proceeding of Residential Workshop on Materials and Methods For Low-Cost Road and Rail and Reclamation Works, Australia, 1976.

[3] G. G. Meyerhof, Bearing Capacity and Settlement of Pile Foundations, Journal of Geotechnical and Geoenvironmental Engineering, 102(3) (1976) 197-228.

[4] A. S. Vesic, Design of Pile Foundations, Transportation Research Board, Washington DC, 1977.

[5] K. Terzaghi, R. B. Peck, G. Mesri, Soil Mechanics in Engineering Practice, John Wiley, New York, 1996.

[6] G. L. Babu, B. S. Murthy, D. S. Murthy, M. S. Nataraj, Bearing Capacity Improvement Using Micropiles: A Case Study, GeoSupport Conference, 2004.

[7] S. Haeri, A. Hamidi, N. Tabatabaee, The Effect of Gypsum Cementation on the Mechanical Behavior of Gravely Sands, Geotechnical Testing Journal, 28(4) (2005) 380-390.

[8] P. J. Sabatini, B. Tanyu, T. Armour, P. Groneck, J. Keeley, Micropile design and construction, FHWA-NHI-05-039, US Department of Transportation Federal Highway Administration, Washington DC, 2005.

[9] M. Sadek, I. Shahrour, H. Mroueh, Influence of micropile inclination on the performance of a micropile network, Proceedings of the Institution of Civil Engineers - Ground Improvement, 10(4) (2006) 165-172.

[10] B. Muhunthan, F. Sariosseiri, Interpretation of Geotechnical Properties of Cement Treated Soils, Research Report WA-RD 715.1 Pullman Washington State University, Washington, 2008.

[11] T. K. Datta, Seismic Analysis of Structures, John Wiley & Sons, Delhi, 2010.

[12] A.Y. Abd Elaziz, M. H. El Naggar, Group behavior of hollow-bar micropiles in cohesive soils, Canadian Geotechnical Journal, 51 (2014) 1139-1150.

[13] Y. Amini, A. Hamidi, E. Asghari, Shear strength–dilation characteristics of cemented sand–gravel mixtures, International Journal of Geotechnical Engineering, 8(4) (2014), 406-413.

[14] K. Abdollahi, A. Mortezaei, A new expression for determining the bending stiffness of circular micropile groups, Soil Dynamics and Earthquake Engineering, 77 (2015) 58-70.

[15] R. P. Matos, P. L. Pinto, C. S. Rebelo, L. S. Silva, M. Veljkovic, Cyclic Performance of Single and Group Micropiles on Loose Sand, IFCEE, 2015.

[16] A.M. Alnuaim, H. El Naggar, H. El Naggar, Numerical investigation of the performance of micropiled rafts in sand. Computers and Geotechnics, 77 (2016) 91-105.

[17] S. Ghadimi, A. Ghanbari, M. Sabermahani, M. Yazdani, Effect of soil type on nail pull-out resistance, Proceedings of the Institution of Civil Engineers - Ground Improvement, 170(2) (2017) 81-88.

[18] S. Rezazadeh, A. Eslami, Empirical methods for determining shaft bearing capacity of semi-deep foundations socketed in rocks, Journal of Rock Mechanics and Geotechnical Engineering, 9(6) (2017) 1140-1151.

[19] A.M. Alnuaim, H. El Naggar, H. El Naggar, Performance of micropiled rafts in clay: Numerical investigation. Computers and Geotechnics, 99 (2018) 42-54.

[20] M. Khanmohammadi, K. Fakharian, Evaluation of performance of piled-raft foundations on soft clay: A case study, Geomechanics and Engineering, 14(1) (2018) 43-50.

[21] J. Ko, J. Cho, S. Jeong, Analysis of load sharing characteristics for a piled raft foundation, Geomechanics and Engineering, 16(4) (2018) 449-461.

[22] D. Kyung, J. Lee, Interpretative Analysis of Lateral Load–Carrying Behavior and Design Model for Inclined Single and Group Micropiles, Journal of Geotechnical and Geoenvironmental Engineering, 144(1) (2018).

[23] D. Kyung, J. Lee, Uplift Load-Carrying Capacity of Single and Group Micropiles Installed with Inclined Conditions, Journal of Geotechnical and Geoenvironmental Engineering, 143(8) (2018).

[24] J. C. Verbrugge, C. Schroeder, Geotechnical Correlations for Soils and Rocks, John Wiley & Sons, 2018.

[25] Sharma, S. Sarkar, Z. Hussain, A Study of Parameters Influencing Efficiency of Micropile Groups, Ground Improvement Techniques and Geosynthetics, 14 (2019) 11-18.

[26] J. M. Schultz, S. Jafroudi, T. V. Nguyen, Verification Load Testing of Micropiles under Combined Axial and Lateral Forces, Eighth International Conference on Case Histories in Geotechnical Engineering, 2019.

[27] Al-abboodi, T. T. Sabbagh, O. Al-salih, Response of passively loaded pile groups – an experimental study, Geomechanics and Engineering, 20(4) (2020) 333-343.

[28] M. Abdlrahem, H. El Naggar, Axial performance of micropile groups in cohesionless soil from full-scale tests, Canadian Geotechnical Journal, 57 (2020).

[29] H. Bayesteh, M. Fakharnia, Numerical simulation load test on hollow-bar micropiles by considering grouting method, Geotechnical Engineering, (2020).